

EXPERIMENTS ON ELECTRON COOLING

G. I. Budker, Ya. S. Derbenev, N. S. Dikansky, V. I. Kudelainen
I. N. Meshkov, V. V. Parkhomchuk, D. V. Pestrikov, B. N. Sukhina
A. N. Skrinsky

Institute of Nuclear Physics
Siberian Division
USSR Academy of Sciences

The electron cooling method was suggested by one of the authors in the middle sixties. The original idea of electron cooling published in 1966¹ is the following: An electron beam is put into one of the straight sections of a storage ring of heavy particles (protons, for example). The average velocity of electrons is the same as that of protons both in amount and direction. Then, in the rest frame system, two beams running through each other are equivalent to a two-component plasma. If the effective electron temperature is low enough, the proton temperature will increase to the electron temperature (when the multiple scattering on the residual gas is not appreciable). That means the angular divergence of the proton beam θ_p is decreased down to the value

$$\theta_p \sim \sqrt{\frac{m}{M}} \theta_e \quad (1)$$

where θ_e is the temperature angular spread of electrons, m is the electron mass, M is the proton mass. Similarly an energy spread in the proton beam is

$$\frac{\Delta E_p}{E} \sim \sqrt{\frac{m}{M}} \beta^2 \gamma \theta_e \quad (2)$$

Damping time is determined by the following expression

$$\tau = \frac{3}{2\sqrt{2}\pi} \left(\frac{mc^2}{e^2} \right) \left(\frac{Mc^2}{e_p^2} \right) \frac{\gamma^2}{n\eta c L} \left[\left(\frac{T_e'}{mc^2} \right)^{3/2} \theta_p \ll \theta_e \quad (3) \right. \\ \left. \theta_p^3 \beta^3 \gamma^3 \theta_p \gg \theta \right]$$

where n is the density of electrons in the laboratory system, T_e' is the electron temperature in the particle system, e and e_p are the electron and proton charges respectively, η is the ratio between the length of the orbit section occupied by the electron beam and its circumference, $L \approx 20$ is the Coulomb logarithm, c is the velocity of light.

Naturally, the cooling process kinetics is more complex. One should take into account the peculiarity of the proton beam motion in a storage ring as well as the effects of mistakes in lining up the average velocities of electrons and protons, the electron beam coherent fluctuations, etc. These questions have been previously studied theoretically^{2,3}, in computer simulations³ and now experimentally.

The experiments were carried out on the special installation^{4,5} called NAP-M (NAP is an abbreviation for "antiproton storage ring", M - model). The installation is schematically shown in Fig. 1 and its general view is given in Fig. 2.

Table I Parameters of the Storage Ring NAP-M

Proton energy	up to 150 MeV
Injection energy	1.5 MeV
Harmonic number	1
Bending radius of magnets	3 m
Straight section length	7.1 m
Aperture of bending magnets:	
vertical	7 cm
radial	10 cm
Interaction region aperture	6 cm

Table I (Continued)

Betatron wave numbers:	
ν_z	1.24
ν_x	1.34
Momentum compaction factor	0.8
Transition energy	110 MeV
Average pressure	$5 \cdot 10^{-10}$ Torr
Acceleration time	30 sec

The electron beam installation (Fig. 3,4) is located in one of the storage ring straight sections and has the parameters given in Table 2.

Table 2 Parameters of the Electron Beam Installation

Interaction region length	1 m
Electron energy	up to 100 keV
Electron current	up to 1 A
Temperature angular spread	$2 \cdot 10^{-3}$
Energy stability	$2 \cdot 10^{-4}$
Longitudinal magnetic field	1 kG

Formation of the intense beam with the small transverse velocities was performed with the special three electrode gun placed into an homogeneous longitudinal magnetic field⁶. The electron energy recovering is used. In the installation the collector potential is higher than the cathode potential by 1-2 kV. The use of electron energy recovering is especially important for the high energy region.

Typical experimental conditions and the best previous results are given in Table 3.

Table 3 Typical Conditions of the Experiment and Main Results

ρ	50 MeV;	50 μ A
e	27 keV	0.1 A
Electron beam temperature		0.2 eV
Temperature angular spread		$2 \cdot 10^{-3}$
Damping time of protons		3 sec
The proton beam equilibrium dimension		1 mm
The proton beam equilibrium angular spread		$\pm 5 \cdot 10^{-5}$
Proton beam momentum spread		10^{-4}
Proton beam lifetime	with electron cooling	5000 sec
	without electron cooling	900 sec

The electron beam temperature was calculated from the damping time and proton beam equilibrium dimension values independently. In the experiments described, the rf system was switched off after acceleration and protons drifted in the constant magnetic field of the storage ring. After acceleration, the longitudinal magnetic field and the cathode heating of the electron beam installation is switched on. It was found that the lifetime of protons is substantially increased in the presence of the electron beam with its optimum energy. The time dependence of the proton current is shown in Fig. 5. Electron losses are due to their scattering on the residual gas. Just after acceleration the proton beam dimensions are small enough and the proton losses are due to single scattering. Some time later the multiple Coulomb scattering makes the beam dimensions increase up to the aperture dimension and

the particle losses increase by a factor of the Coulomb logarithm (in our case by a factor of 5). However, if the electron beam is switched on, the multiple scattering is suppressed and the equilibrium dimension is achieved. The lifetime being determined, as initially, by a single scattering.

Several methods were used for measurements of the proton beam dimensions. At present the most convenient way is that using the magnesium thin jet. The jet crosses the proton beam and the secondary electrons are collected by an electrostatic field and registered by the scintillation screen and photomultiplier. In the experiments the jet with its transversal dimensions $1 \times 20\text{mm}$ moved vertically and the large dimension of the "band" was oriented along the beam direction, the magnesium vapour pressure in the jet being 10^{-6}Torr . The signal is proportional to the proton vertical dimension about 1mm as shown in Fig. 6. If now one switches the electron beam off, then in a large enough time the peak is "diffused" so that the small remaining signal corresponds to an enlarged proton beam. At repeated switching on of the electron beam the same peak reappears, i.e. protons are damped to 1mm (in a time needed for cooling).

Using the method described one can obtain the time dependence for the proton beam current density at the certain vertical coordinate. Fig. 7 shows the oscilloscope traces of the beam density with time in the beam center after the inflector kick. The signal level at point 1 corresponds to increased dimensions of the beam and region 2 shows the beam compression and the particle density increase in the center of the beam, point 3 is the signal level out of the beam.

All the effects connected with the beam cooling can be observed only on the condition that the proton velocities after acceleration differ from the electron velocities in magnitude by not more than $1 \cdot 10^{-3}$. The cooling process has certainly a lot of detail but it is impossible to describe them in this paper. Their description will be published later.

A few remarks on the possible application of electron cooling.

Naturally, the most important possibility arising now is the accumulation of intense and compressed antiproton beam for various purposes. It is possible to enumerate several classes of experiments in physics in which performance possibilities appeared with the successful test of electron cooling (Table 4).

1. The proton-antiproton interaction study in the range of high and super high energies with colliding beams of high luminosity⁷.

2. The use of high monochromaticity of cooled proton and antiproton beams for investigation of narrow resonances (ψ type).

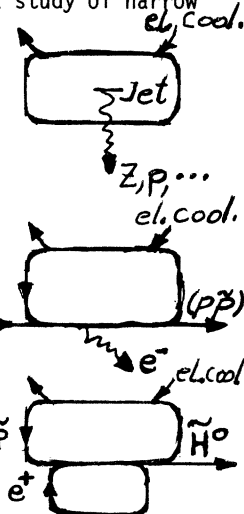
3. Spectrometric experiments on super thin inner targets with the cooled beams of heavy particles.

4. The antiproton beams accumulating with intensity high enough in the region of low energies (on the order of several MeV). In this case it becomes feasible to investigate (in pure conditions) the proton-antiproton bound state (protonium). High efficiency transformation of 100% of antiprotons into protonium can be obtained by putting together the antiproton beam and the beam of hydrogen atoms travelling parallel to the antiproton beam with the same average velocity.

5. It is also possible to generate antihydrogen atom formation by recombination of antiprotons with positrons. The latter idea seems to be quite capable of realization at present. The neutral hydrogen production in NAP-M at recombination of protons with cooling electrons is about 10^{-3} .

Table 4 Possible Applications of Electron Cooling

1. $p\text{-}\bar{p}$ - high energies, high luminosity;
2. $p\text{-}\bar{p}$ - high monochromaticity, a study of narrow resonances (ψ type);
3. Spectrometric experiments with inner targets
4. A study of proton-antiproton bound state in experiments with antiprotons of low energies (on the order of several MeV);
5. Antihydrogen generation in experiments with antiprotons of low energy.



Indeed, there are also some other possible electron cooling applications.

REFERENCES

1. G. I. Budker, Rep. on Intern. Conf. at Orsay, 1966, "Atomnaya Energia", 22, 1967.
2. Ya.S.Derbenev, A.N. Skrinsky, "Kinetics of Electron Cooling in Storage Rings of Heavy Particles," Prepr. N255 Nucl. Phys. Inst. Siberian Division USSR Academy of Sciences, Novosibirsk, 1968.
3. G. I. Budker et al., "Kinetics of Electron Cooling," Report on IV National Conf. on Accelerators of Charged Particles, Moscow, 1974.
4. V. V. Anashin et al., "Installation for Experiments on Electron Cooling", Report on IV National Accelerator Conference, Moscow, 1974.
5. G. I. Budker et al., "First Experiments on Electron Cooling", Report on IVth National Accelerator Conference, Moscow, 1974.
6. V. I. Kudelainen, I. N. Meshkov, R. A. Salimov, "Journal of Techn. Phys.", 41, 2294. 1971.
7. "Proton-Antiproton Colliding Beams", Report of VAP-NAP Group, Nucl. Phys. Inst. Siberian Division of the USSR Academy of Sciences, Proceedings of 8th Intern. Conf. on High Energy Accelerators, CERN, Geneva, 1971.

ACKNOWLEDGEMENT

The authors wish to express their thanks to all the staff of the Institute whose efforts ensured the success of this work.

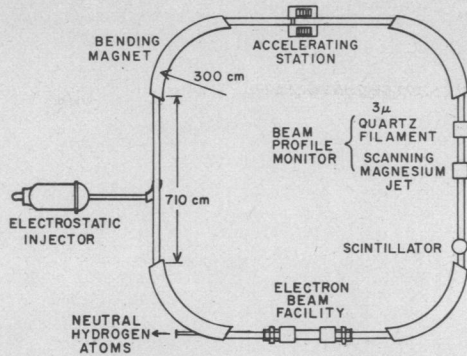


Fig. 1 - The NAP-M storage ring layout.



Fig. 2 - General view of storage ring NAP-M

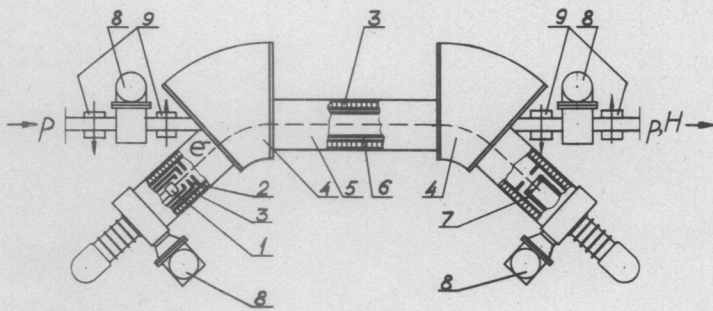


Fig. 3 - The electron beam installation layout:
 1-electron gun, 2 anodes, 3-solenoid coils,
 4-electron beam bending region, 5-interaction region, 6-vacuum chamber, 7-collector, 8-vacuum pumps, 9-correction magnets.

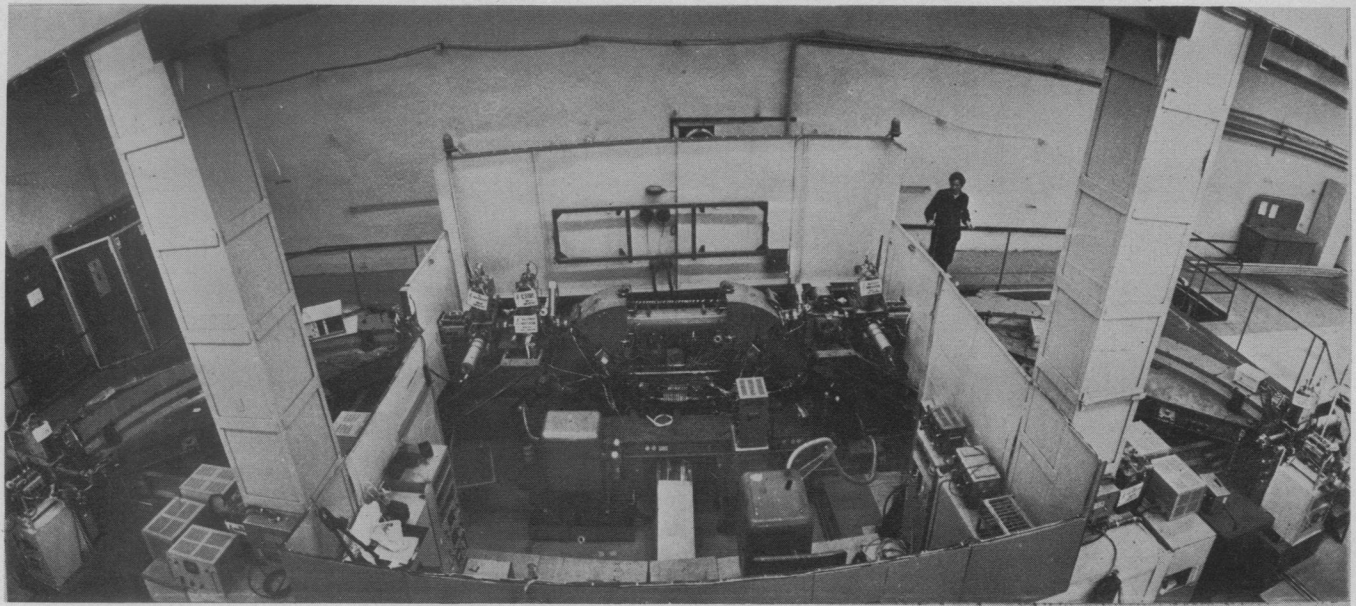


Fig. 4 - General view of the electron beam installation.

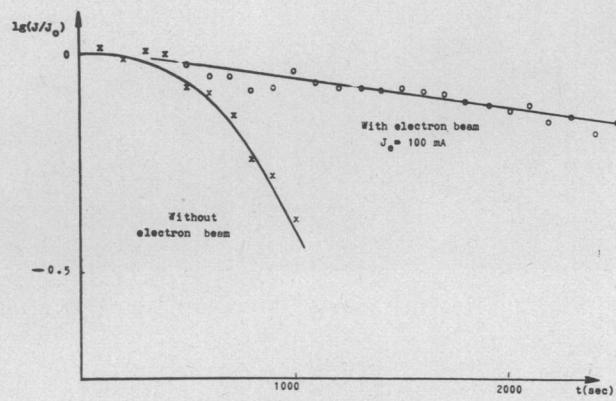
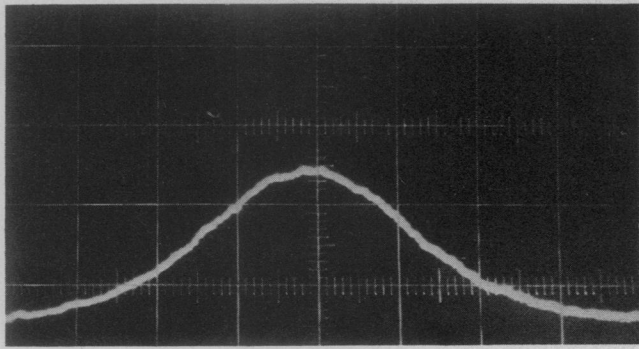
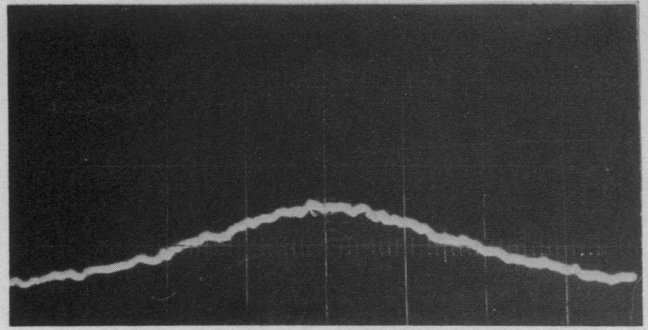


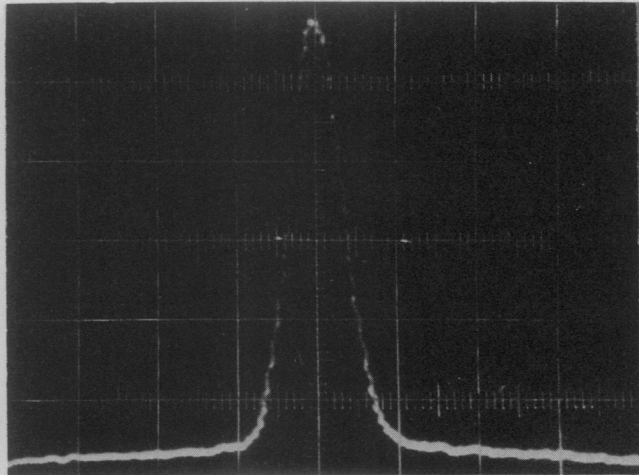
Fig. 5 - Time dependence for the proton current.



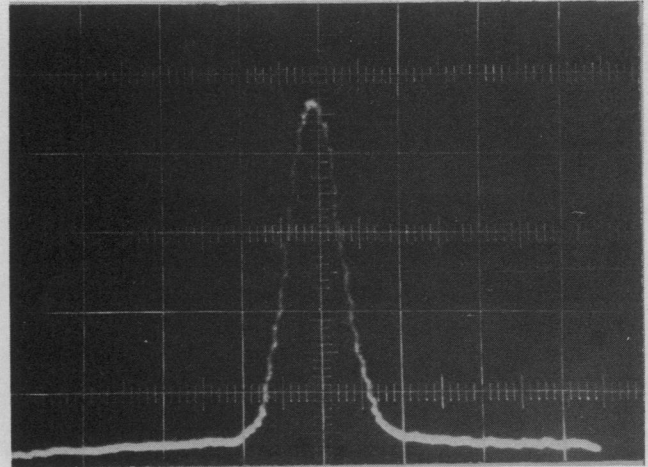
6a - proton beam just after acceleration, electron beam switching on;



6c - preliminary cooled proton beam in 200 sec after electron beam switching off;

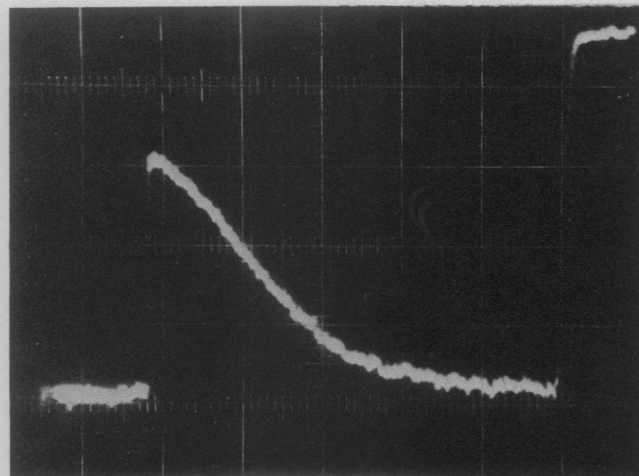


6b - proton beam in 10 sec after electron beam switching on;



6d - beam (Fig. c) after the electron beam repeated switching on in 10 sec. Scale 1 mm/Division.

Fig. 6 - Oscilloscope trace of the vertical distribution of protons:



1 2 3

Fig. 7 - Oscilloscope trace of the density change with time in the center of the proton beam:

- 1-beam dimension is enlarged by the inflector kick;
- 2-beam compression during cooling;
- 3-signal level out of the beam. Scanning time 2 sec/cm.